National Conference with International Participation
ENGINEERING MECHANICS 2001
Svratka, Czech Republic, May 14 – 17, 2001

MACROSCOPIC APPROACH TO STRESS ANALYSIS OF AORTIC ANEURYSM

Eduard Rohan*, Robert Cimrman†

Summary: *In this paper we try to analyze numerically mechanical behaviour of the abdominal aneurysmatic aorta (AAA). For this we apply the composite model of smooth muscle which has been developed by authors and described in [1, 2]. Several geometrical parameters are considered to define various shapes of AAA. For these the tensions in collagen and elastin fibres are evaluated.*

Key words: *abdominal aortic aneurysm, composite model, fibrous stress, anisotropy, elastin, collagen, finite elements.*

1 Introduction

The abdominal aortic aneurysm AAA, cf. [3], is a result of chronic degenerative conditions associated with aging, atherosclerosis, male gender, hypertension and other phenomena. From normal aorta the AAA differs in the shape and the material properties. The wall of normal aorta consists of three distinguishable layers — intima, media and adventitia. The two "boundary" layers, i.e. intima and adventitia, are less important in the context of strength and stress transmission. Intima is formed mainly by endothelial and fibroblast cells. Adventitia contains collagen connective tissues which are very compliant, connecting aorta with surrounding organs. The pulsatile arterial blood pressure is balanced mainly by the media layer with the largest thickness of the three ones (approx. 1 mm), consisting of about 60 elastic perforated membranes separated by smooth muscle cells (SMC) and collagen fibres. The membranes are formed by elastin fibres abundant in spiral grids

The AAA is a product of pathological processes which may have different origins and causes in particular occurrences. In contrast with normal aorta the tissue of AAA seems to be organized chaotically. Media of normal aorta contains approximately 40–60 % of elastin, 12–20 % of collagen, the rest constituted by SMC (about 40 %). In media of AAA elastin is low distributed (0–30 %) being replaced by collagen (45–55 %), the volume fraction of SMC is decreased. These figures, however, are only tentative and may depend on the stage of AAA, cf. [3]. Aneurysms evolve through three clinical stages. Stage I (early aneurysm) is characterized by elastin degradation and by increased production of collagen; the maximum diameter of AAA is 2–3 cm. In stage II collagen degradation (the change of the collagen type, or annihilation) is balanced by collagen production; the maximum diameter of AAA is up to 5 cm. Stage III is "unstable", characterized by accelerated collagen degradation exceeding its production. If AAA expands over 5 cm, the risk of rupture is quite serious and generally the surgical repair is required in this stage.

The obvious reason for a surgical operation of AAA is to prevent its rupture. The simple 5 cm diameter based criterion has proved to be insufficient in practice. Also other geometrical characteristics determining the shape of AAA should be considered to justify operation in some

*Dr. Ing. Eduard Rohan, Department of Mechanics, Faculty of Applied Sciences, University of West Bohemia, Univerzitní 22, 306 14 Plzeň; tel. +420 19 7491121, e–mail: rohan@kme.zcu.cz

†Ing. Robert Cimrman, New Technologies Research Center, University of West Bohemia, Univerzitní 22, 306 14 Plzeň; tel. +420 19 7491586, e–mail: cimrman3@ntc.zcu.cz

particular instances. The critical state of AAA should be correlated with values of mechanical wall stress. In [4] the stress analysis of AAA was based on linear elastic isotropic material assuming small deformation. The bulge shape of the vessel was parametrized by a maximum diameter and an excentricity of the aneurysm. It was shown that both these parameters influence peak stresses, however, because of the rough simplifications of the biological material (the linear analysis) a stronger conclusions could not be made.

The purpose of the present paper is to carry out a similar analysis of the stress response of AAA. For this we apply the composite model of smooth muscle which has been developed by the authors and described in [1, 5]. A brief summary of the model is presented in the following section.

2 Composite model of arterial wall

The model is based on the mixture theory approach. The microstructure of the smooth muscle tissue is characterized by volume fractions of the three basic components involved: the *active fibres* representing bundles of muscle cells, the *passive fibres* corresponding to collagen, elastin fibres and the *matrix*. In aneurysmatic aortic wall the mechanical importance of SMCs is suppressed, as they are minor in comparison with other components (collagen, elastin). Nevertheless, activation of SMC is constant, persisting in the "pseudo-passive" ("latch") regime. Due to this fact in our computational model we omit the presence of the muscle fibres substituting bundles of SMCs and use a simplified model comprising only passive fibres (elastin and collagen) and the hyperelastic matrix.

We consider three constituents of the reduced model: elastin, collagen and matrix. Their respective volume fractions are denoted by ϕ_e, ϕ_c and ϕ_m, where $\phi_e + \phi_c + \phi_m = 1$. They remain constant during deformation. At any point of the continuum the model enables both the elastin and collagen fibres to be distributed in several preferential directions in which the tension can be transmitted — the k^{th} one is denoted by ν_i^k in the undeformed configuration, $k \in I^e$ for the elastin fibres, $k \in I^c$ for the collagen ones; I^e, I^c are index sets. A quantity of fibres in the k^{th} direction is proportional to the volume fraction ϕ_n^k, $\sum_{k\in I^n} \phi_n^k = 1$ for $n = e, f$. Introducing the directional tensor (in the reference configuration)

$$\omega_{ij}^k = \nu_i^k \nu_j^k \ , \tag{1}$$

we can express the fibre stresses as follows:

$$\tau_{ij}^e = \sum_{k\in I^e} \phi_e^k \tau_e^k \omega_{ij}^k \ , \quad \tau_{ij}^c = \sum_{k\in I^c} \phi_c^k \tau_c^k \omega_{ij}^k \ , \tag{2}$$

the fibre tensions τ_e^k, τ_c^k are defined using elastic and viscoelastic models, respectively. The matrix is defined using the neo-Hookean hyperelastic model. By C_{ij} we denote the right Cauchy-Green deformation tensor, $J = (\det(C_{ij}))^{1/2}$, $E_{ij} = \frac{1}{2}(C_{ij} - \delta_{ij})$. Using the above notation we can write the total 2^{nd} Piola-Kirchhoff stress:

$$S_{ij} = -JC_{ij}^{-1} p + \phi_m \frac{\partial W^m}{\partial E_{ij}} + \phi_e \tau_{ij}^e + \phi_c \tau_{ij}^c \ . \tag{3}$$

The first term involving the thermodynamic pressure p results from the assumed genuine incompressibility of the bulk composite material, the second one is the stress in the hyperelastic matrix (the gradient of the strain energy w.r.t. Green-Lagrange strain E_{ij}). Projecting E_{ij} in the direction of a fibre we obtain strain in the fibre, i.e. $\epsilon^k = E_{ij}\omega_{ij}^k$, see (1). Based on this we define the tensions of (2)

$$\text{elastin:} \quad \tau_e^k = \mathcal{E}_e(\epsilon^k - \bar{\epsilon}_e^k), \quad k \in I^e \ , \tag{4}$$

$$\text{collagen:} \quad \sigma_c^k = \mathcal{E}_c[\exp\{\kappa(\epsilon^k - \bar{\epsilon}_c^k)\} - 1], \quad k \in I^c \ , \tag{5}$$

where σ_c is the elastic response stress of the viscoelastic model of collagen fibres, see [2, 1], so that for the relaxed state one has $\tau_c^k = (1-\gamma)\sigma_c^k$. By $\bar{\epsilon}_e^k < 0$ for $k \in I^e$ we account for prestraining of elastin fibres, whereas for collagen fibres we usually take $\bar{\epsilon}_c^k > 0$, $k \in I^c$ to account for collagen waviness in unloaded state.

3 Geometry of AAA

For our numerical simulations we take a model of AAA with length $L = 11$ cm and the nominal diameter $d = 2$ cm, see Fig. 1. The bulge shape is described by the following parameters: maximal diameter of the midsection $D_{\max}$ (the distance between anterior and posterior walls), the width of the midsection $D_{\min}$, excentricity parameter e, oblateness o. The transverse sections of the vessel are described by ellipses derived by a nonlinear interpolation between end-circles and the midsection ellipse with the axes $D_{\max}$, $D_{\min}$; if $o = 1$, then $D_{\min} = D_{\max}$, if $o = o_{\min}$, then $D_{\min} < D_{\max}$ such that the circle with diameter $d = 2$ cm osculates the ellipse at its "anterior" and "posterior" points. Concerning the wall thickening of the mid part the three cases are considered: case 0 — constant thickness 0.26 cm for the whole vessel, case A — uniform thickening at the mid part, case B — thickening along the anterior part of the surface, normal thickness at the posterior past. The maximum thickness in cases A, B is $t_{\max} = 0.26 \cdot (1 + t_r)$, for t_r see Tab. 1.

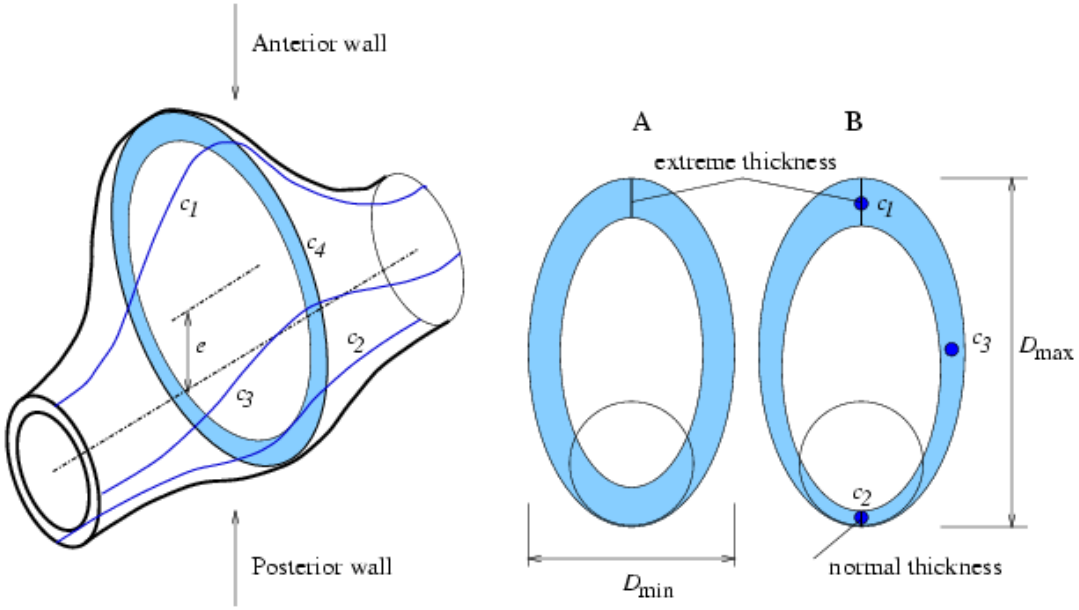

Fig. 1: Scheme of AAA geometry: c_1–c_4 are curves of stress evaluation, by A, B are labeled the two cases of thickening.

4 Material parameters

We assumed that both collagen and elastin fibres are distributed in preferential directions; at any point of the mid-surface of the arterial shell in the tangent plane we define two spiral fibres, $\underline{\nu}^1$, $\underline{\nu}^2$, declined 10° off the circumferential direction and one longitudinal direction $\underline{\nu}^3$, so that $I^e = I^c = \{1, 2, 3\}$. In the normal part of the vessel (the ends) we take $\phi_e^1 = \phi_e^2 = 0.15$, $\phi_e^3 = 0.20$, $\phi_c^1 = \phi_c^2 = 0.1$, $\phi_c^3 = 0.05$, whereas in the midsection we take $\phi_e^1 = \phi_e^2 = \phi_e^3 = 0.05$, $\phi_c^1 = \phi_c^2 = 0.25$, $\phi_c^3 = 0.2$, see (2). Further we define $\bar{\epsilon}_e^k = -0.14$ and $\bar{\epsilon}_c^k = 0.1$, $k = 1, 2, 3$ at the ends, whereas $\bar{\epsilon}_e^k = -0.14$, $k = 1, 2, 3$ and $\bar{\epsilon}_c^k = -0.06$ is used in the midsection. The parameters $\bar{\epsilon}_e^k$, $\bar{\epsilon}_c^k$ vary linearly with the "radial" coordinate; the above values are defined on

the outer surface of the vessel, whereas we have $\bar{\epsilon}_e^k, \bar{\epsilon}_c^k = 0$ on the inner surface. This variation should account for the well-known prestraining of arterial walls, see e.g. [6].

The constitutive laws for elastin and collagen in (4), (5) are defined with $\mathcal{E}_e = 2 \cdot 10^3$ kPa, $\mathcal{E}_c = 50$ kPa, $\kappa = 13$, the viscoelasticity of collagen is given by the relaxation parameter $\gamma = 0.75$, and $T_{\text{relax}} = 1$ s.

type:	01	02	03	04	05	06	07	08	09	10	11	12	13	14
$D_{\max}$	4.5	4.5	4.5	4.5	4.5	4.5	3.5	3.5	3.5	3.5	3.5	3.5	5.5	5.5
e	1.25	1.25	1.25	1.25	0.75	0.75	0.75	0.75	0.75	0.75	0.35	0.35	1.25	1.75
o	1	$o_{\min}$	1	$o_{\min}$	1	$o_{\min}$	1	$o_{\min}$	1	$o_{\min}$	1	$o_{\min}$	1	$o_{\min}$
T	0	0	A	B	A	B	0	0	A	B	A	B	A	B
t_r	0	0	1.3	1.3	1.3	1.3	0	0	1.0	1.0	0.9	0.9	1.3	1.3

Tab. 1: Geometrical parameters of the AAA types 01 – 14.

5 Results

The numerical simulations were performed for fourteen types of the AAA geometry, see Tab. 1, labeled as 01 – 14. Each model of the vessel was fixed in axial the direction on the "left" end, the mesh points of the "right" one were restricted to have a same axial displacement. The results are introduced for maximal arterial pressure load 25 kPa applied gradually in 1 s, starting at unloaded relaxed state.

In order to assess the strength of the particular AAA cases we evaluated tensions in both elastin and collagen fibres along material curves c_1–c_4, see Fig. 1, defined on the mid-surface of the shell. Curve c_1 is on the anterior side, c_2 is on the posterior one, while c_3 is on the lateral side; c_4 is the transversal section of the mid-shell. Figs. 4–9 present the Cauchy (true) tension in collagen fibres in the spiral (fibres 1) and longitudinal (fibres 2) directions for types 01–06, i.e. $D_{\max} = 4.5$ and 13, 14, i.e. $D_{\max} = 5.5$. Similar results for elastin are in Figs. 10–13. For $D_{\max} = 3.5$ a selection of results is in Figs. 15–20. In Figs. 2, 3 we present comparison of the unloaded and loaded vessel for $D_{\max} = 5.5$. Figs. 21–34 show tension in collagen spiral fibres in the inflated geometry.

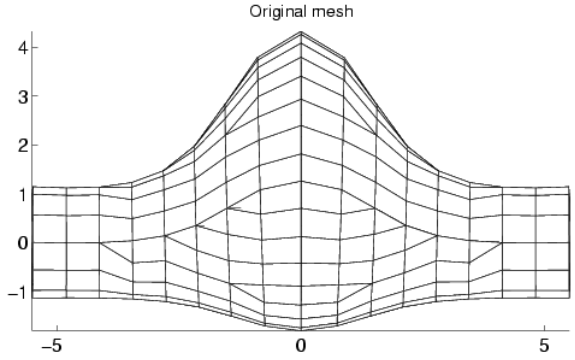

Fig. 2: Original mesh, case 13.

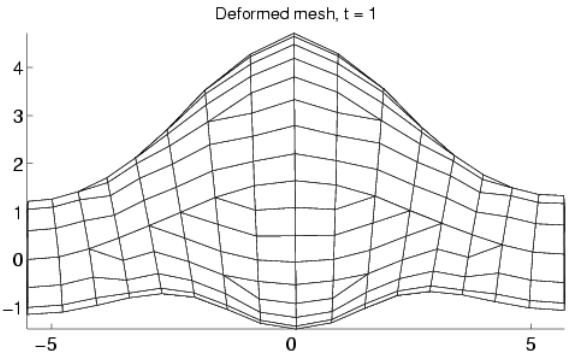

Fig. 3: Deformed mesh, case 13.

6 Conclusion

In the numerical tests we observed that, in general, the behaviour of the vessel depends strongly on the material data, namely on the choice of the fibre directions and the prestraining. Of particular interest are the boundary conditions prescribed at the ends of the vessel. In [4] the clamped ends were used, thus causing an axial stress. In contrast with it we assumed that no axial force is transmitted by the vessel and, simultaneously, the vessel does not elongate significantly when inflated. For this, however, we had to tune the material topology data.

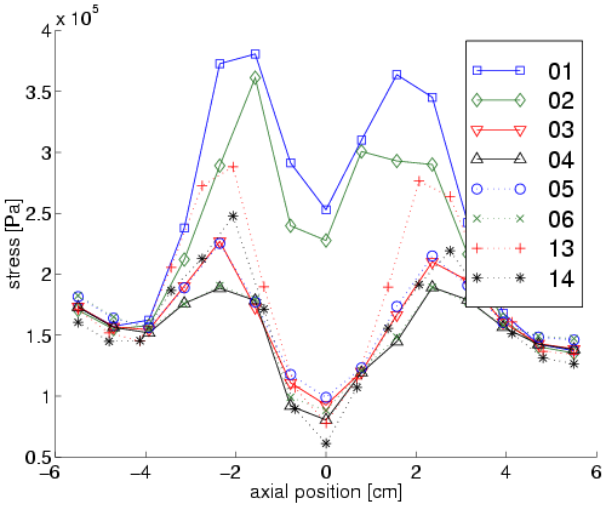

Fig. 4: Collagen fibres 1, curve 1.

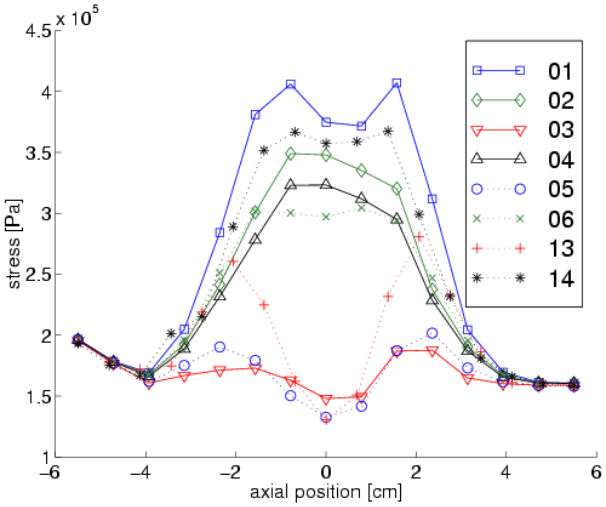

Fig. 5: Collagen fibres 1, curve 2.

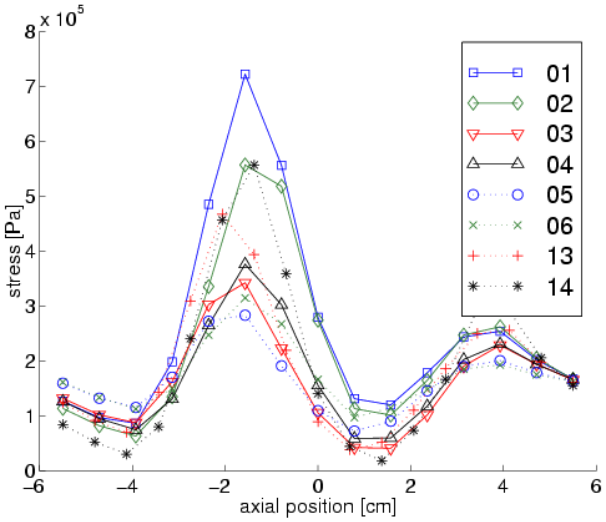

Fig. 6: Collagen fibres 1, curve 3.

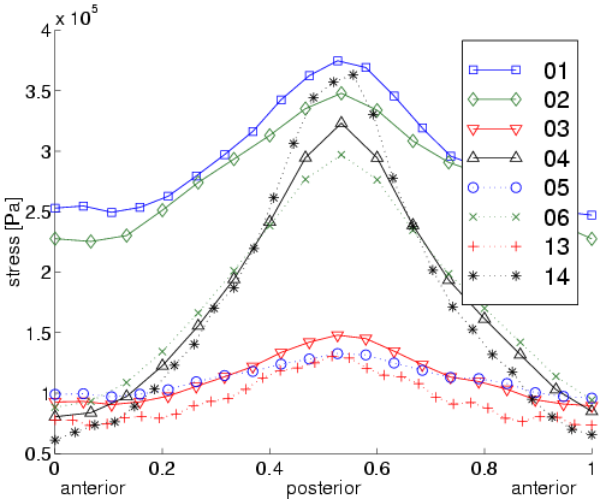

Fig. 7: Collagen fibres 1, curve 4.

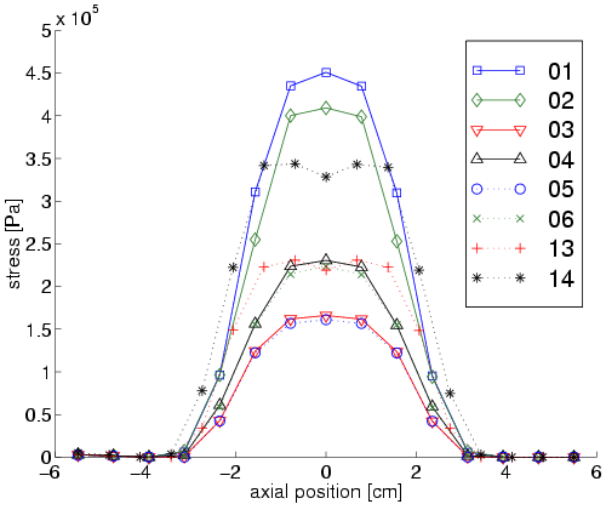

Fig. 8: Collagen fibres 3, curve 3.

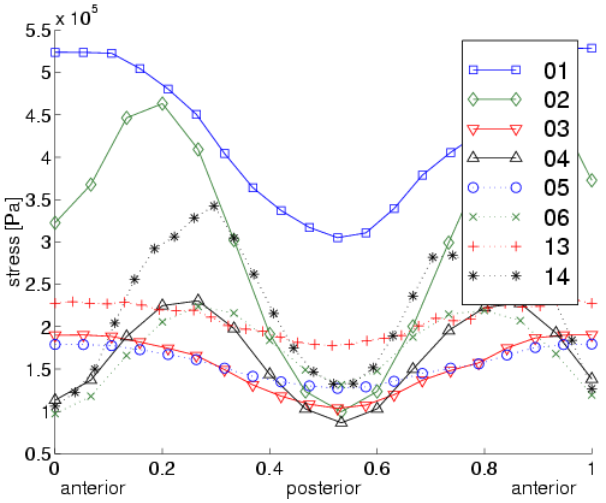

Fig. 9: Collagen fibres 3, curve 4.

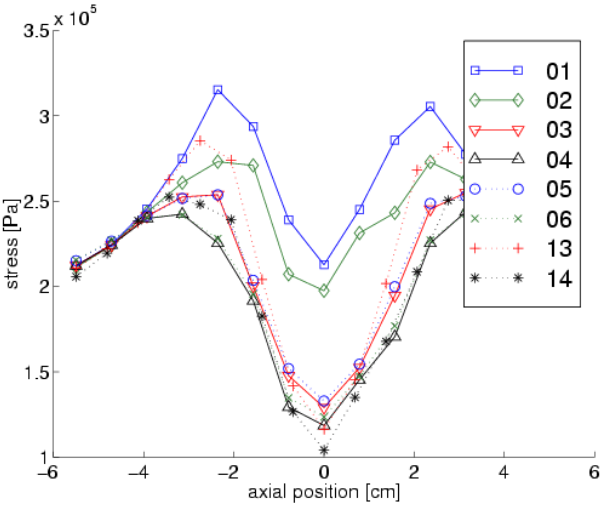

Fig. 10: Elastin fibres 1, curve 1.

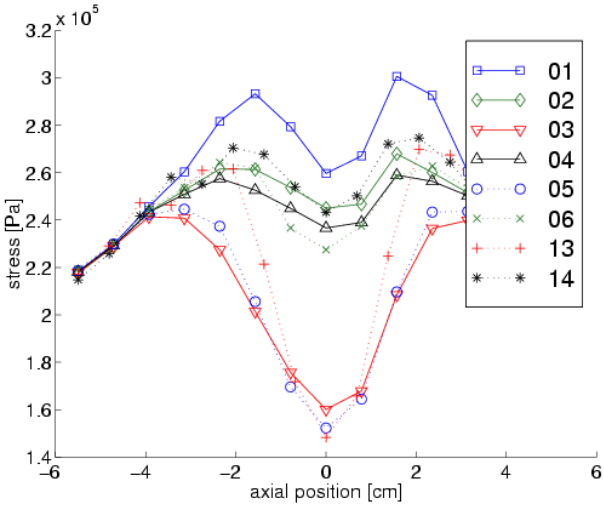

Fig. 11: Elastin fibres 1, curve 2.

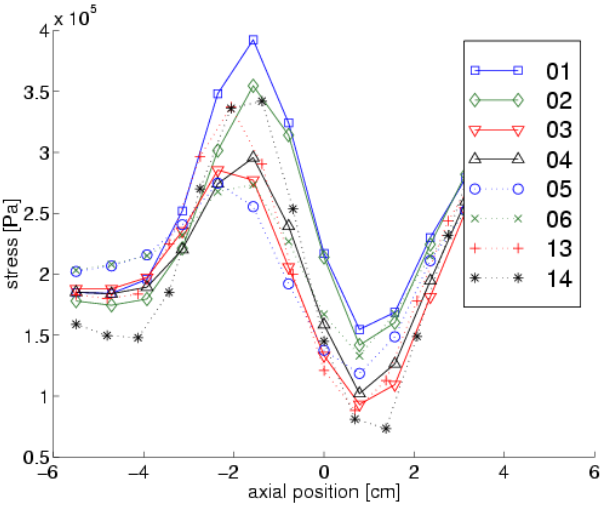

Fig. 12: Elastin fibres 1, curve 3.

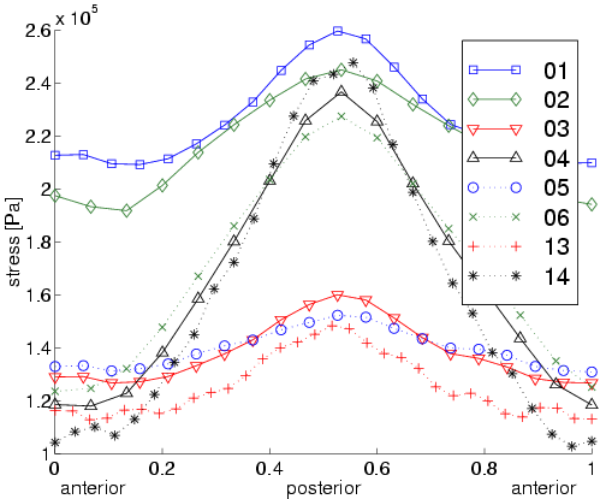

Fig. 13: Elastin fibres 1, curve 4.

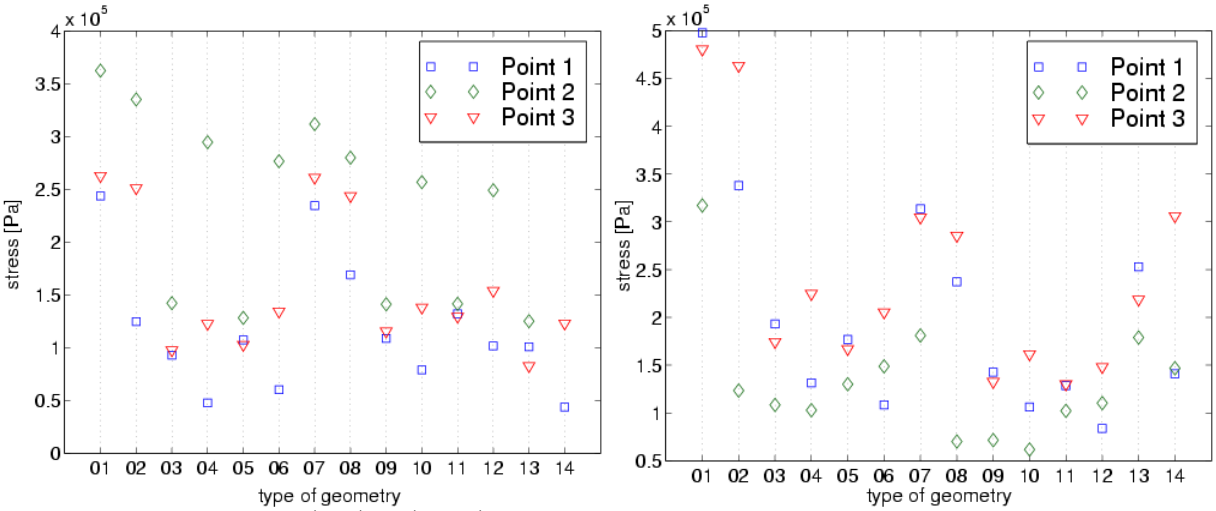

Fig. 14: Collagen fibres 1 (left), 3 (right) — all tests. Points 1–3 are intersections of the midsection with the curves c_1–c_3, respectively.

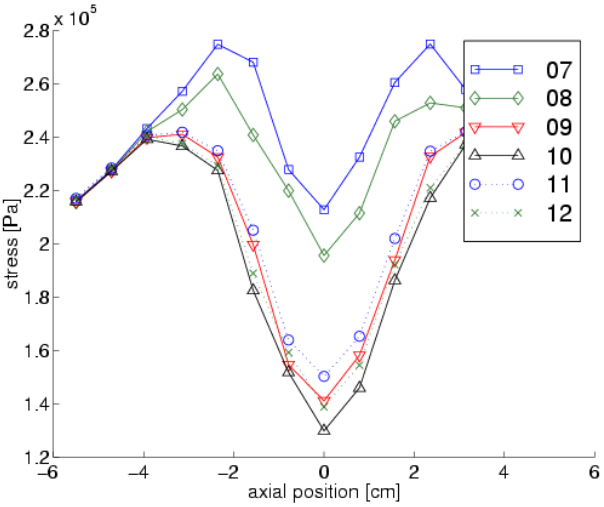

Fig. 15: Elastin fibres 1, curve 1.

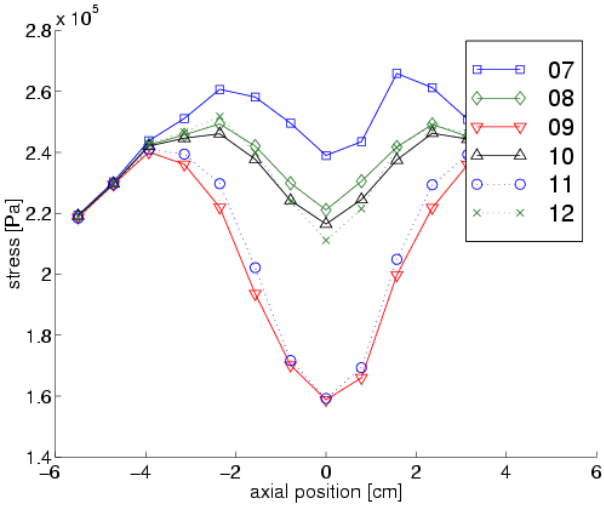

Fig. 16: Elastin fibres 1, curve 2.

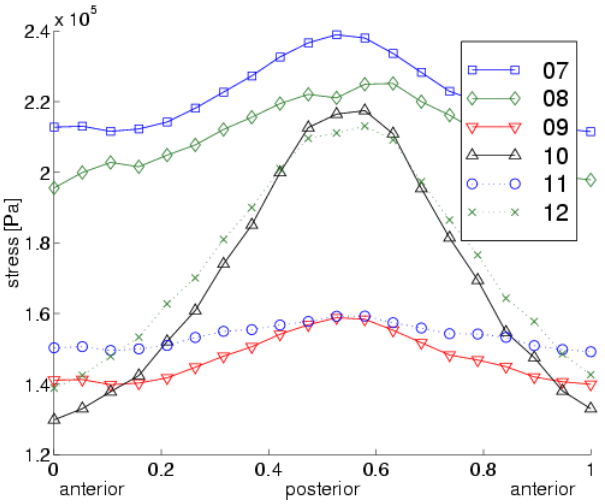

Fig. 17: Elastin fibres 1, curve 4.

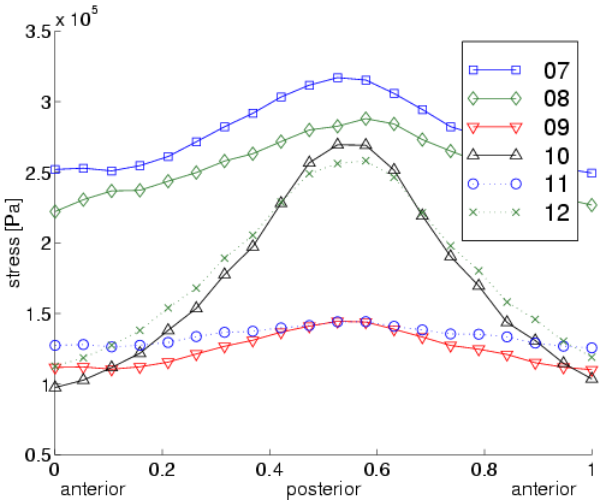

Fig. 18: Collagen fibres 1, curve 4.

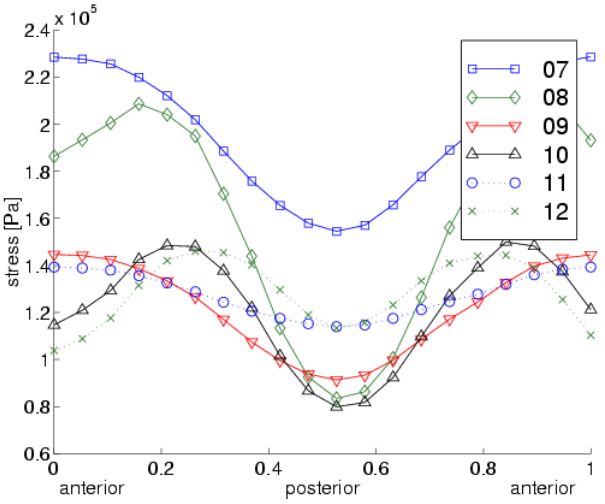

Fig. 19: Elastin fibres 3, curve 4.

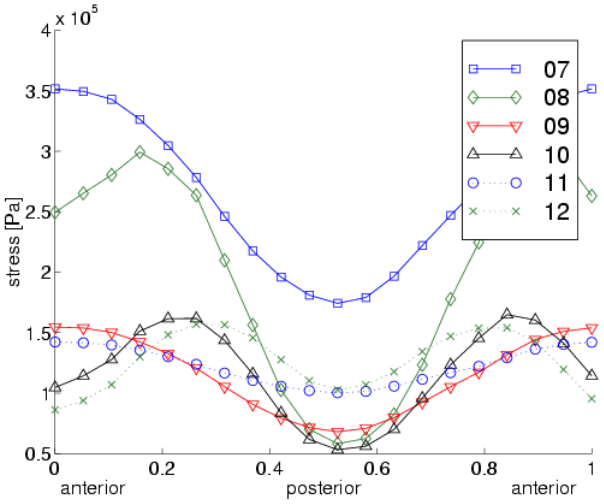

Fig. 20: Collagen fibres 3, curve 4.

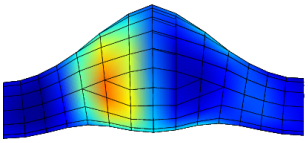

Fig. 21: Case 01.

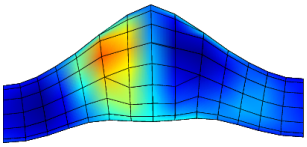

Fig. 22: Case 02.

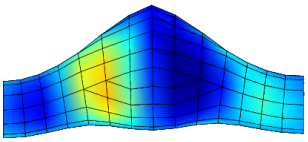

Fig. 23: Case 03.

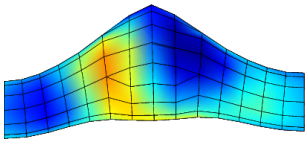

Fig. 24: Case 04.

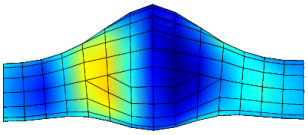

Fig. 25: Case 05.

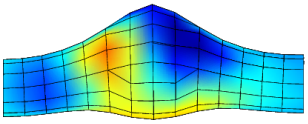

Fig. 26: Case 06.

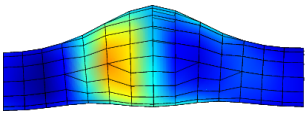

Fig. 27: Case 07.

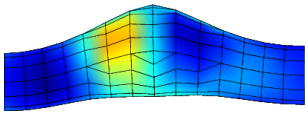

Fig. 28: Case 08.

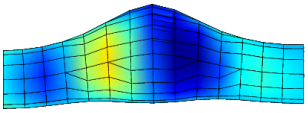

Fig. 29: Case 09.

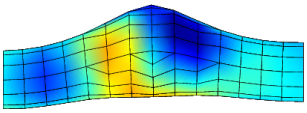

Fig. 30: Case 10.

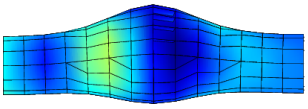

Fig. 31: Case 11.

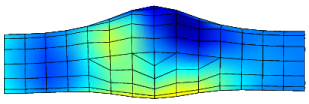

Fig. 32: Case 12.

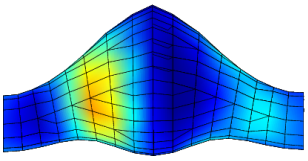

Fig. 33: Case 13.

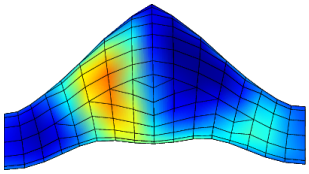

Fig. 34: Case 14.

The interpretation of the given figures is not easy. On the other hand we may conclude, that the thickness of the posterior wall is important parameter as well as the oblateness of the midsection. These parameters were not considered in [4]. In some cases the worst tensile loading is not in the mid-section. Therefore, we suggest to evaluate stresses along the four curves c_1–c_4, see Fig. 1. Some objective comparison of all the analyzed types of AAA can be found in Fig. 14.

Acknowledgements: This paper was supported by the project LN00B084 of the New Technologies Research Center of the University of West Bohemia in Plzeň.

Reference

[1] E. Rohan and R. Cimrman. Sensitivity analysis and material identification for activated smooth muscle. In *Proceedings of the conference Numerical Methods in Continuum Mechanics 2000*, pages 143–144, Liptovský Ján, Slovak Republic. (2000). Full version on CD-ROM.

[2] E. Rohan and R. Cimrman. Optimization methods in material identification for composite model of resting smooth muscle. In *Proceedings of the conference Engineering Mechanics 2000*, volume III, pages 59–64, Svratka. (2000).

[3] V. Třeška, A. Ferko, I. Chytra, J. Kočová, A. Krajina, and B. Kreuzberg. *Aneuryzma břišní aorty.* Grada Publishing, Praha, (1999).

[4] D.A. Vorp, M.L. Raghavan, and M.W. Webster. Mechanical wall stress in abdominal aortic aneurysm: Influence of diameter and asymmetry. *Journal of vascular surgery*, **27**(4), 632–639, (1998).

[5] E. Rohan and R. Cimrman. Numerical simulation of activated smooth muscle behaviour using finite elements. In *Proceedings of UWB*, pages 143–155, Plzeň. University of West Bohemia in Plzeň, (2000).

[6] Y.C. Fung. *Biomechanics. Mechanical Properties of Living Tissues.* Springer-Verlag, New York, second edition, (1993).